Single-channel monitoring of reversible L-type Ca^{2+} channel $Ca_V\alpha_1$-$Ca_V\beta$ subunit interaction

Wanchana Jangsangthong,[†‡Δ] Elza Kuzmenkina, [†Δ] Ann Kristin Böhnke, [†‡] and Stefan Herzig,[†‡*]

[†] *Department of Pharmacology and* [‡] *Center for Molecular Medicine, University of Cologne, Germany*

[Δ] *Wanchana Jangsangthong and Elza Kuzmenkina contributed equally to this work.*

*** *Correspondence:*** *Department of Pharmacology,University of Cologne, Gleueler Str 24, 50931 Köln, Germany, email:* *Stefan.herzig@uni-koeln.de*

SUPPORTING MATERIAL

MATERIALS AND METHODS

Construction of expression vectors for L-type Ca^{2+} channel auxiliary subunits

cDNA coding sequence of human full-length $Ca_V\beta_{1a}$ subunit (GeneBank accession #M92301) was excised from pIRES2-EGFP-β_{1a} (1) by SacI and BamHI endonucleases and inserted into SacI and BamHI sites of pIRES2-DsRed2 (Clonetech, Mountain view, CA, USA) to generate pIRES2-DsRed2-β_{1a}. Human full-length $Ca_V\beta_{2b}$ subunit (GeneBank accession #AF285239) was encoded by bicistronic expression vector pIRES2-EGFP-β_{2b} (2). cDNA encoding human $Ca_V\alpha_2\delta1$ subunit (GeneBank accession #NM_00722) was excised from plasmid pcDNA3.1/Hygro-$\alpha_2\delta1$ (kindly provided by Prof. Dr. Lehmann-Horn) (3) by digestion with BamHI and NotI and, then, subcloned into the BamHI and NotI sites of vector pIRESpuro3 (Clonetech, Mountain view, CA, USA), yielding expression vector pIRESpuro3-$\alpha_2\delta1$.

Cell culture and transfection

HEK293α_{1C} cell line stably expressing human cardiac $Ca_V1.2$ subunit (GeneBank #NM_000719) was a generous gift of Dr. Gyula Varadi (4). HEK293α_{1C} cells were cultured and co-transfected with auxiliary subunits as described previously (1, 5). Here, $Ca_V\alpha_2\delta1$ subunit and either $Ca_V\beta_{1a}$, $Ca_V\beta_{2b}$ or a mixture of both $Ca_V\beta$ subunits were used. For transfection, pIRESpuro3-$\alpha_2\delta1$ was mixed with either pIRES2-DsRed2-β_{1a}, pIRES2-EGFP-β_{2b} or the mixtures of pIRES2-DsRed2-β_{1a} and pIRES2-EGFP-β_{2b} in 3:1 ratio by DNA mass (i.e., 4.5 µg of pIRESpuro3-$\alpha_2\delta1$ was applied along with 1.5 µg of plasmids encoding $Ca_V\beta$ subunits). For competition experiments, pIRES2-DsRed2-β_{1a} and pIRES2-EGFP-β_{2b} were mixed in 2:1 or 1:1 ratios by plasmid DNA mass (i.e., 1 µg of pIRES2-DsRed2-β_{1a} and 0.5 µg of pIRES2-EGFP-β_{2b} for mixture 2:1, and 0.75 µg of both pIRES2-DsRed2-β_{1a} and pIRES2-EGFP-β_{2b} for mixture 1:1). For mock-transfections (β^{-}), mixture of pIRES2-DsRed2 and pIRES2-EGFP plasmids (1:1 ratio by DNA mass) was used instead of plasmids encoding $Ca_V\beta$ subunits. In addition to the procedures described in (1), 24 h after transfection, cells were cultured under the normal growth condition in selective medium (complete culture medium containing geneticin and puromycin (both from PAA, Pasching, Austria) at final

concentrations of 500µg/ml and 3 µg/ml, respectively) in 35 mm Petri dishes (Falcon, Heidelberg, Germany) to ensure selecting of the fluorescent cells that express $Ca_V\alpha_2\delta1$ subunit.

Whole-cell current analysis

To calculate peak current density, the *I-V* data from each cell were fitted with a Boltzmann-Ohm equation: $I_V = G_{max} (V-V_{rev})/(1+\exp[(V_{0.5,act} - V)/k_{act}])$ where I_V is the current density at the test voltage V, G_{max} is the maximum conductance density, $V_{0.5,act}$ is the mid-point of voltage dependence of activation, V_{rev} is the reversal potential, and k_{act} is the slope factor. For more accurate evaluation of the voltage dependence of the activation, Ba^{2+} tail currents were elicited by repolarizing to –50 mV for 10 ms after a 20 ms test pulse between -50 and +80 mV from the holding potential (applied every 5 s). Amplitudes of the tail currents were fitted with the Boltzmann function: $I_{max}/(1+\exp[(V_{0.5,act} - V)/k_{act}])$ where I_{max} is the maximum tail current. To obtain the voltage dependence of the steady-state inactivation, cells were depolarized from a holding potential to conditional pre-pulses from –110 to +40 mV for 5 s, after which they were depolarized to a test potential of +10 mV for 125 ms (applied every 30 s). Current amplitudes were fitted with the Boltzmann function: $I_{max}/(1+\exp[(V_{inact} - V_{0.5,inact})/k_{inact}])$ where I_{max} is the maximum current amplitude, V_{inact} is the conditional potential, $V_{0.5,inact}$ is the mid-point of voltage dependence of inactivation, and k_{inact} is the slope factor. Kinetics of the current inactivation were estimated by determination of the percentage of Ba^{2+} currents that have inactivated after either 150 ms or 5 s of depolarization.

qRT-PCR

qRT-PCR was performed to identify the presence of endogenous $Ca_V\beta_1$, $Ca_V\beta_2$, $Ca_V\beta_3$, and $Ca_V\beta_4$ subunits as well as the pore-forming $Ca_V\alpha_{1C}$ subunits in HEK293 and HEK293α_{1C} cells. Cells were harvested from culture and not more than 7×10^6 cells where used for RNA extraction. Total RNA was isolated from individual samples using RNeasy Mini Kit (Qiagen, Hilden, Germany) according to manufacturers' protocols. RNA concentration was measured using NanoDrop 2000C (Thermo Scientific, Wilmington, DE, USA) and first-strand cDNA was synthesized from 200 ng of total RNA using QuantiTect reverse transcription kit (Qiagen, Hilden, Germany) according to manufacturer’s guidelines. 1 µl of reverse transcription reaction (10 ng cDNA) was used for quantitative analysis by qRT-PCR, with primers specific

for human $Ca_V\beta_1$, $Ca_V\beta_2$, $Ca_V\beta_3$, $Ca_V\beta_4$ and $Ca_V\alpha_{1C}$; glyceraldehyde 3-phosphate dehydrogenase (GAPDH) was used as reference gene (primer sequences are listed in Table S1). PCR Master Mix containing Quanti Tect SYBR Green (Qiagen, Hilden, Germany), primer concentrations of 0.5 μM and cDNA were prepared according to manufacturers' protocols. Reactions were run on a Lightcycler (Roche Applied Science, Basel, Switzerland) with 15 min initial denaturation at 95 °C, then thermo cycled at 95 °C for 15 s, 58 °C for 25 s, and 72 °C for 10 s for 35 cycles, followed by melting curve analysis. Δct values were calculated from differences between GAPDH and the different subunits of Ca_V channels.

SUPPORTING REFERENCES

1. Jangsangthong, W., E. Kuzmenkina, I. F. Khan, J. Matthes, R. Hullin, and S. Herzig. 2010. Inactivation of l-type calcium channels is determined by the length of the n terminus of mutant beta(1) subunits. *Pflugers Arch.* 459:399-411.
2. Hullin, R., J. Matthes, S. von Vietinghoff, I. Bodi, M. Rubio, K. D'Souza, I. Friedrich Khan, D. Rottlander, U. C. Hoppe, P. Mohacsi, E. Schmitteckert, R. Gilsbach, M. Bunemann, L. Hein, A. Schwartz, and S. Herzig. 2007. Increased expression of the auxiliary beta(2)-subunit of ventricular l-type ca(2)+ channels leads to single-channel activity characteristic of heart failure. *PLoS One*. 2:e292.
3. Schleithoff, L., G. Mehrke, B. Reutlinger, and F. Lehmann-Horn. 1999. Genomic structure and functional expression of a human alpha(2)/delta calcium channel subunit gene (cacna2). *Genomics*. 61:201-209.
4. Schultz, D., G. Mikala, A. Yatani, D. B. Engle, D. E. Iles, B. Segers, R. J. Sinke, D. O. Weghuis, U. Klockner, M. Wakamori, and et al. 1993. Cloning, chromosomal localization, and functional expression of the alpha 1 subunit of the l-type voltage-dependent calcium channel from normal human heart. *Proc Natl Acad Sci U S A*. 90:6228-6232.
5. Hullin, R., I. F. Khan, S. Wirtz, P. Mohacsi, G. Varadi, A. Schwartz, and S. Herzig. 2003. Cardiac l-type calcium channel beta-subunits expressed in human heart have differential effects on single channel characteristics. *J. Biol. Chem.* 278:21623-21630.

TABLES

TABLE S1 qRT-PCR primer sequences.

Gene human	Gene ID	Sequence
$Ca_V\beta_1$	CACNB1	F 5’-AAT GTT GGC TAC AAT CCG TCT C-3’ R 5’-CCG ATC CAC CAG TCA TTA TTG T-3’
$Ca_V\beta_2$	CACNB2	F 5’-CAA CGT CCA GAT GGT AGC AG-3’ R 5’-CTC CAG ATA GTC GGC AAG GT-3’
$Ca_V\beta_3$	CACNB3	F 5’-GTC CTC CCA GTG CCA TCC-3’ R 5’-ATC AGA GGG CAT CAA GCT GT-3’
$Ca_V\beta_4$	CACNB4	F 5’-CAC CAT ATC CCA CAG CAA TTT-3’ R 5’-AGT TCT CTG TGG AGT GGT TGC T-3’
$Ca_V\alpha_{1C}$	CACNA1c	F 5’-CAC GAT CTT CAC CAA CCT GA-3’ R 5’-CTG AAG GAG GTG TGC TGG A-3’
Glyceraldehyde 3-phosphate dehydrogenase	GAPDH	F 5’-CAT GTT CGT CAT GGG TGT GAA CCA-3’ R 5’-ATG GCA TGG ACT GTG GTC ATG AGT-3’

TABLE S2 Peak current density and voltage dependence of channel activation and inactivation.

Gating parameter	$Ca_V\beta_{1a}$	$Ca_V\beta_{1a}Ca_V\beta_{2b}$ (2:1)	$Ca_V\beta_{1a}Ca_V\beta_{2b}$ (1:1)	$Ca_V\beta_{2b}$	β^-
Peak current density [pA/pF]	$-52.0 \pm 3.8^{\dagger}$ $n = 9$	$-60.2 \pm 1.6^{\dagger}$ $n = 8$	$-56.7 \pm 2.6^{\dagger}$ $n = 6$	$-61.5 \pm 6.6^{\dagger}$ $n = 6$	-14.5 ± 2.9 $n = 5$
$V_{0.5,act}$ [mV]	$-23.5 \pm 0.9^{\dagger,\ddagger}$ $n = 8$	$-15.8 \pm 1.0^{\dagger}$ $n = 7$	$-15.9 \pm 2.5^{\dagger}$ $n = 3$	$-13.2 \pm 1.2^{\dagger}$ $n = 5$	3.0 ± 1.7 $n = 5$
$V_{0.5,inact}$ [mV]	$-41.1 \pm 1.0^{\dagger,\ddagger}$ $n = 8$	$-40.3 \pm 1.5^{\dagger,\S}$ $n = 5$	$-38.4 \pm 2.0^{\dagger}$ $n = 5$	$-35.1 \pm 1.1^{*}$ $n = 6$	-29.1 ± 2.5 $n = 4$

Maximum Ba^{2+} currents and parameters of voltage dependent activation and inactivation of $Ca_V1.2$ channels modulated by $Ca_V\beta_{1a}$ subunit, mixture $Ca_V\beta_{1a}Ca_V\beta_{2b}$ (2:1), mixture $Ca_V\beta_{1a}$ $Ca_V\beta_{2b}$ (1:1), or $Ca_V\beta_{2b}$ subunit in HEK293α_{1C} cells. Voltage of half-maximum activation ($V_{0.5,act}$) and voltage of half-maximum steady-state inactivation ($V_{0.5,inact}$) were obtained from fitting of normalized tail current amplitudes and steady-state inactivation curves, respectively. All values are given as mean ± SE.

$*$ and † for statistics, $p \leq 0.05$ and $p \leq 0.01$ compared with $Ca_V1.2$ channels from mock-transfected cells (β^-) (one-way ANOVA followed by Dunnett´s post-test).

‡ and § for statistics, $p \leq 0.01$ and $p \leq 0.05$ compared with $Ca_V1.2$ channels containing β_{2b}-subunits (one-way ANOVA followed by Dunnett´s post-test).

TABLE S3 Single-channel gating parameters.

Gating parameter	$Ca_V\beta_{1a}$	$Ca_V\beta_{1a}Ca_V\beta_{2b}$ (2:1)	$Ca_V\beta_{1a}Ca_V\beta_{2b}$ (1:1)	$Ca_V\beta_{2b}$	β^-
Availability [%]	$60.8 \pm 3.6^{\dagger}$	64.7 ± 3.3	77.0 ± 7.0	82.7 ± 5.3	52.3 ± 7.1
$P_{(O)}$ [%]	$0.39 \pm 0.1^{\dagger}$	0.58 ± 0.2	0.83 ± 0.3	1.19 ± 0.2	0.28 ± 0.1
Peak current [fA]	$-4.7 \pm 1.1^{\dagger}$	-6.4 ± 1.8*	-9.2 ± 3.2	-14.2 ± 2.0	-4.3 ± 1.2
Inactivation [%]	$64.3 \pm 7.2^{\dagger}$	$62.4 \pm 2.8^{\dagger}$	34.2 ± 8.2	29.5 ± 3.8	36.0 ± 4.8
Mean first latency [ms]	45.3 ± 2.1	43.9 ± 4.1	35.0 ± 4.6	33.5 ± 4.9	55.9 ± 2.7
Mean open time [ms]	0.19 ± 0.01	0.16 ± 0.01	0.20 ± 0.02	0.23 ± 0.02	0.17 ± 0.01
Mean closed time [ms]	20.4 ± 1.3*	15.8 ± 2.3	15.2 ± 2.5	13.1 ± 1.6	24.3 ± 2.4
n =	9	5	4	8	7

The effect of $Ca_V\beta_{1a}$ subunit, $Ca_V\beta_{2b}$ subunit or the $Ca_V\beta_{1a}Ca_V\beta_{2b}$ mixtures on single-channel properties of recombinant $Ca_V1.2$ channels in HEK293α_{1C} cells. Availability: fraction of active sweeps, containing at least one channel opening, $P_{(O)}$: open probability within active sweeps, peak current: peak value of single-channel average current, inactivation: 100% – (relative current remaining at the end of pulse, expressed as percentage of peak current), mean first latency, open times and closed times are simple arithmetic mean values.

* and † for statistics, $p \leq 0.05$ and $p \leq 0.01$ compared with $Ca_V1.2$ channels containing $Ca_V\beta_{2b}$ subunit (one-way ANOVA followed by Dunnett´s post-test).

FIGURES

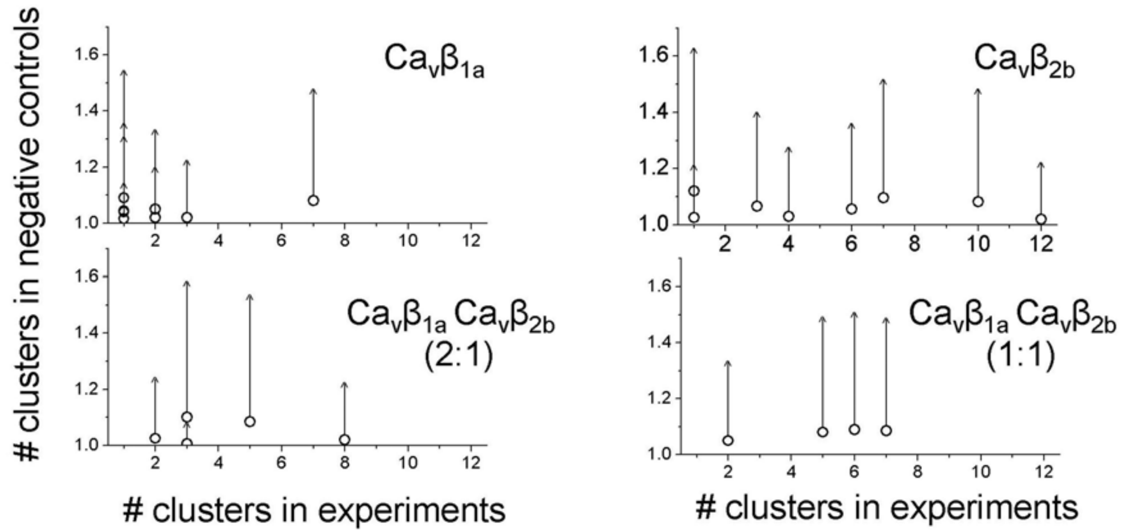

FIGURE S1 Validation of the clustering procedure for single-channel open-probability diaries. For every experiment, 200 randomized open-probability diaries were generated as negative controls and subjected to a clustering procedure. For all experiments, the fraction of randomized open-probability diaries, which were split into two or more clusters, was less than 5%. Open circles show mean + SD of simulations versus true data values for every experiment.

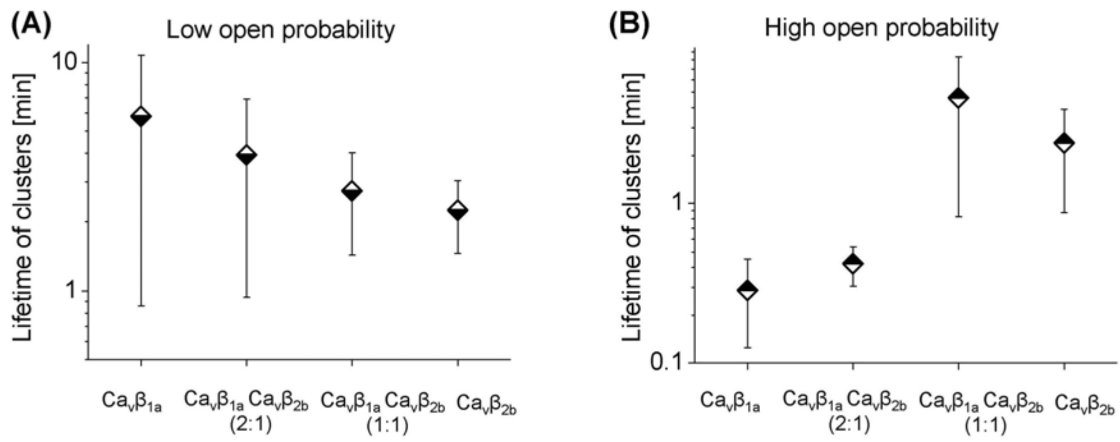

FIGURE S2 Lifetimes of low- and high-open-probability clusters. Mean lifetimes were determined as described in *Materials and Methods*. Errors were estimated by the jackknife method.

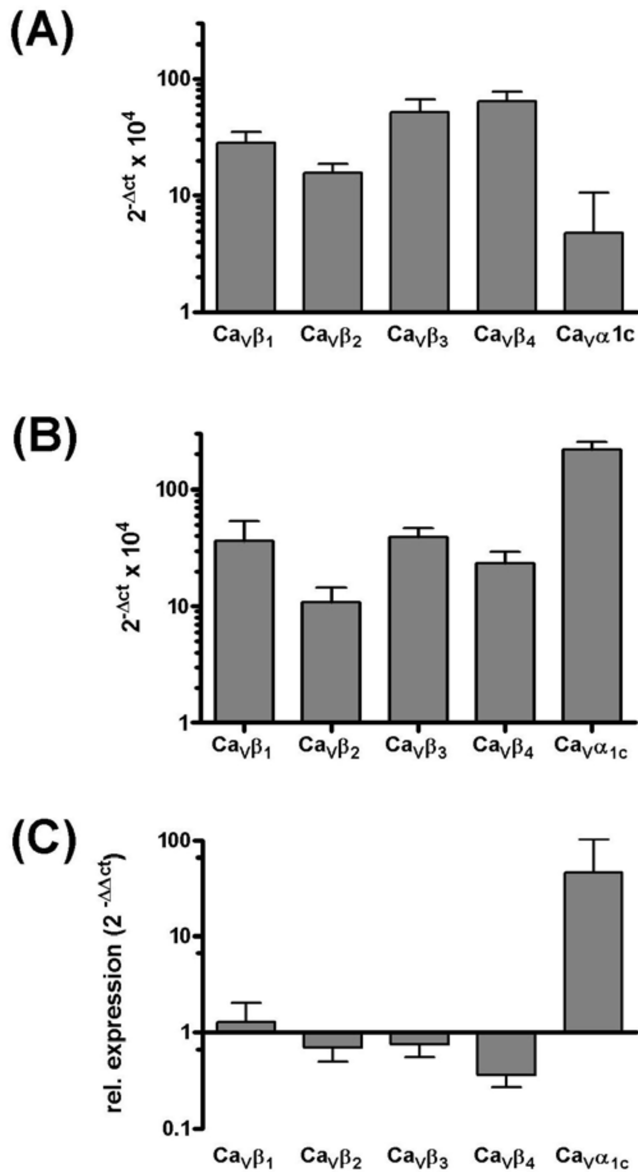

FIGURE S3 Expression of Ca_V subunits in HEK293 and HEK293α_{1C} cells. qRT-PCR was used to quantitatively analyze the mRNA expression of endogenous $Ca_V\beta_1$, $Ca_V\beta_2$, $Ca_V\beta_3$ and $Ca_V\beta_4$ subunits as well as the pore-forming $Ca_V\alpha_{1C}$ subunit. (*A*)–(*B*) $Ca_V\beta_{1\text{-}4}$ subunits and pore-forming $Ca_{V\alpha 1C}$ subunits were found on the mRNA level in native HEK293 (*A*) and HEK293α_{1C} (*B*) cells. Samples were measured in duplicates with n=5 for HEK293 cells and n=3 for HEK293α_{1c} cells using GAPDH as a reference gene. $2^{-\Delta ct}$ values are shown as geometrical mean + SE. (*C*) Relative expression of Ca_V subunits in HEK293α_{1C} cells compared to native HEK293 cells is given as $2^{-\Delta\Delta ct}$ values. Data are shown as geometrical mean + SE. Significant differences are marked by *$p<0.05$ (Student's t-test of Δct values).